Rapid Development of Piperidine Carboxamides as Potent and Selective Anaplastic Lymphoma Kinase Inhibitors

Marian C. Bryan,[†] Douglas A. Whittington,[‡] Elizabeth M. Doherty,[†] James R. Falsey,[†] Alan C. Cheng,[‡] Renee Emkey,[‡] Rachael L. Brake,[‡] and Richard T. Lewis*,[‡]

[†]Medicinal Chemistry Research Technologies, Amgen Inc., One Amgen Center Drive, Thousand Oaks, California 91320, United States

[‡]Amgen Inc., 360 Binney Street, Cambridge Massachusetts 02142, United States

Ⓢ Supporting Information

ABSTRACT: Piperidine carboxamide **1** was identified as a novel inhibitor of anaplastic lymphoma kinase (ALK enzyme assay IC_{50} = 0.174 μM) during high throughput screening, with selectivity over the related kinase insulin-like growth factor-1 (IGF1R). The X-ray cocrystal structure of **1** with the ALK kinase domain revealed an unusual DFG-shifted conformation, allowing access to an extended hydrophobic pocket. Structure–activity relationship (SAR) studies were focused on the rapid parallel optimization of both the right- and left-hand side of the molecule, culminating in molecules with improved potency and selectivity over IGF1R.

ALK IC_{50}	0.174 μM
IGF1R IC_{50}	4.61 μM
Karpass-299 IC_{50}	0.384 μM

1
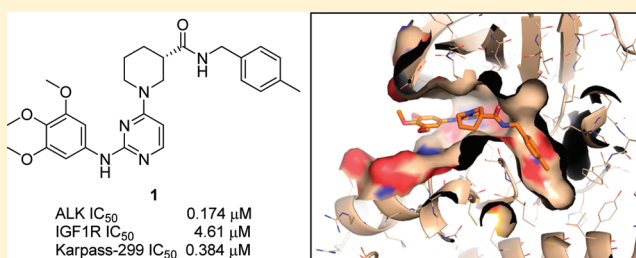
INTRODUCTION

Anaplastic lymphoma kinase (ALK) is a member of the insulin receptor superfamily of tyrosine kinases.[1] Although not widely expressed in adult tissue, ALK is implicated in neuronal development, differentiation, and basal dopaminergic signaling.[2,3] ALK is a putative oncogene and is expressed as part of aberrant fusion proteins in a number of cancers including anaplastic large-cell lymphomas (ALCL), inflammatory myofibroblastic tumors (IMT) and, more recently, a variety of solid tumor types.[1,4] Additionally, abnormal expression of full-length ALK may play a role in oncogenesis given its aberrant expression in a number of different tumor types including diffuse large B-cell lymphoma, neuroblastoma, rhabdomyosarcomas, glioblastomas, and esophageal squamous cell carcinomas.[1,5–8] In these settings, ALK is believed to support tumorigenesis through a variety of signaling mechanisms leading to cell-cycle progression, survival, cell migration, and cell shaping.[9] Recently, the use of crizotinib for the targeted inhibition of ALK has been shown effective in early phase clinical trials against advanced non-small-cell lung cancers carrying activated ALK kinase.[10] Coupling these compelling results with the knowledge that the protein is not widely expressed in adult tissue presents ALK as an attractive oncology target with a potentially large therapeutic window.

We identified piperidine carboxamide **1** (Scheme 1) from a high-throughput screen of our proprietary sample collection against a recombinant, truncated ALK enzyme construct. Compound **1** inhibited the ALK construct with an IC_{50} = 0.174 μM and demonstrated comparable functional activity in a whole cell assay monitoring ALK phosphorylation (IC_{50} = 0.384 μM in ALK-positive Karpas-299 cells).[11] The compound

also exhibited moderate to excellent selectivity over the related kinase family member insulin-like growth factor-1 (IGF1R, IC_{50} = 4.61 μM).[12–14] Selectivity over IGF1R was of particular interest due to its critical functions as a mediator of cell proliferation, differentiation, and apoptosis, and broad expression of this kinase in normal tissue.[15]

Determination of the cocrystal structure of **1** bound to the ALK kinase domain (Figure 1) provided insights into possible improvements in potency and selectivity (PDB ID 4DCE).[16] The cocrystal structure of **1** with ALK shows a "DFG-shifted" conformation, similar to a type 1 1/2 inhibitor conformation.[17] When **1** is bound, Phe1271 of the DFG sequence, which normally occupies a hydrophobic pocket in the apoprotein,[18] shifts and forms a lid on top of the benzyl group, allowing for an edge–face interaction with **1** and access to the extended hydrophobic pocket flanked by Phe1174 and Ile1179 (Figure 1A,B). The carboxamide carbonyl hydrogen bonds to catalytic Lys1150, which also hydrogen bonds to Glu1167. The amide NH, in turn, accepts a hydrogen bond from the backbone carbonyl of Gly1269, the residue preceding the DFG sequence. Additional interactions were observed between hinge residue Met1199 and N1 of the aminopyrimidine ring and the anilinic NH (Figure 1A). Finally, the trimethoxyphenyl group sat in a narrow groove sandwiched by Leu1122 and the hinge region.

Comparison of the cocrystal structure of ALK with **1** and a crystal structure of a benzimidazole inhibitor-bound IGF1R[19] shows residue differences in the region adjacent to the benzyl ring (Leu1196 vs Met1049 and Ile1171 vs Met1024 in IGF1R

Scheme 1. Retrosynthetic Analysis of 1
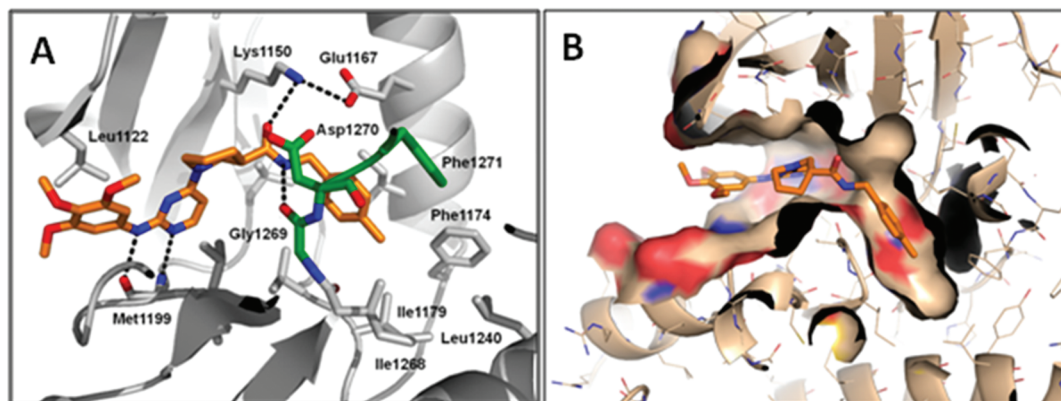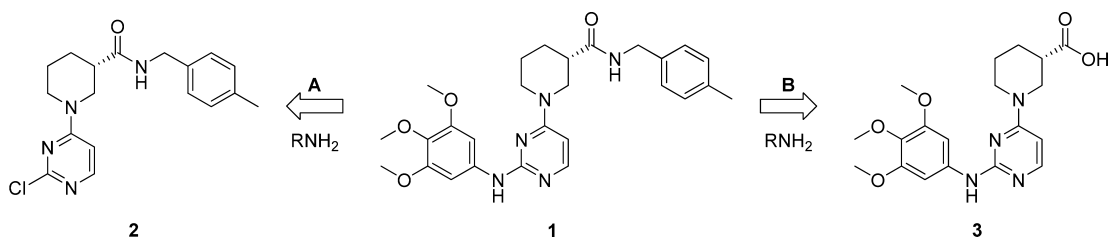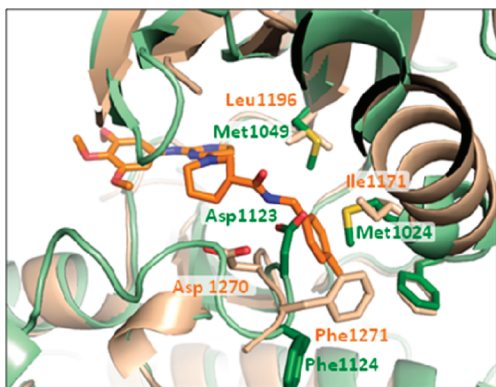

Figure 1. (A) Co-crystal structure of **1** with ALK at 2.0 Å resolution highlighting key interactions with the DFG residues (shown in green). (B) Co-crystal structure of **1** with ALK illustrating the extended hydrophobic pocket. (PDB ID 4DCE).

and ALK, respectively) as well as conformational differences in the DFG region (Figure 2).[20] In the IGF1R crystal structure,

Figure 2. Overlay of cocrystal structures of compound **1** with ALK (PDB ID 4DCE) and a structure of IGF1R bound to a benzimidazole inhibitor (PDB ID 2OJ9). ALK is in brown, **1** is in orange, and IGF1R is in green.

Phe1124 of the DFG region is flipped away from the pocket, precluding a putative favorable stacking interaction with the

benzyl ring of compound **1**. In addition, Asp1123 is oriented inward, where it impinges on the binding of compound **1**. Substitution of Ile1171 (ALK) with Met1024 (IGF1R) also narrows the entrance to the pocket and modifies its shape.

On the basis of these observations, we synthesized a series of analogues designed to probe the extended hydrophobic pocket and the linker binder region to optimize nonbonded interactions while maintaining or improving selectivity over IGF1R.

■ CHEMISTRY

Retrosynthetic analysis of **1** (Scheme 1) reveals a lead amenable to a modular, parallel-synthesis approach. Arrays of analogues were prepared either via S$_N$Ar with chloropyrimidine intermediate **2** (route A, Scheme 1) or by amide coupling to carboxylic acid intermediate **3** (route B, Scheme 1).

Chloropyrimidine **2** was prepared from (S)-1-(tert-butoxycarbonyl)piperidine-3-carboxylic acid (**4**) and p-tolylmethylamine (**5**) according to Scheme 2. HATU-mediated coupling of **4** with **5** provided intermediate **6**. Cleavage of the Boc protecting group under acidic conditions followed by reaction with 2,4-dichloropyrimidine afforded predominantly the desired 4-substituted key intermediate **2**. The three steps

Scheme 2. Synthesis of Compounds 7a−l via Chloropyrimidine Intermediate 2[a]
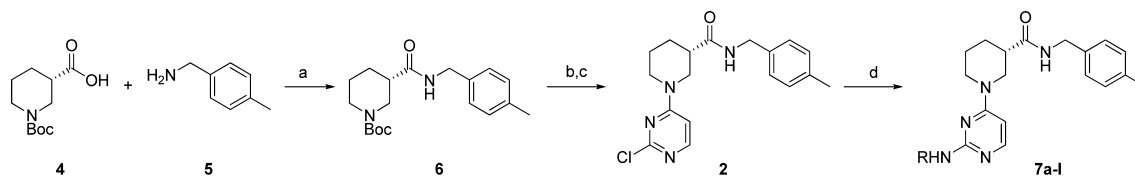
[a]Reagents and conditions: (a) Et$_3$N, HATU, CH$_2$Cl$_2$, 22 °C, 70%; (b) 1 M HCl, CH$_2$Cl$_2$, 22 °C, quant; (c) 2,4-dichloropyrimidine, Et$_3$N, EtOH, 22 °C, 32%; (d) DMSO, 90 °C.
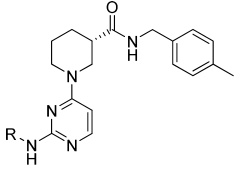
Scheme 3. Synthesis of Compounds 11a–v via Carboxylic Acid Intermediate 3[a]
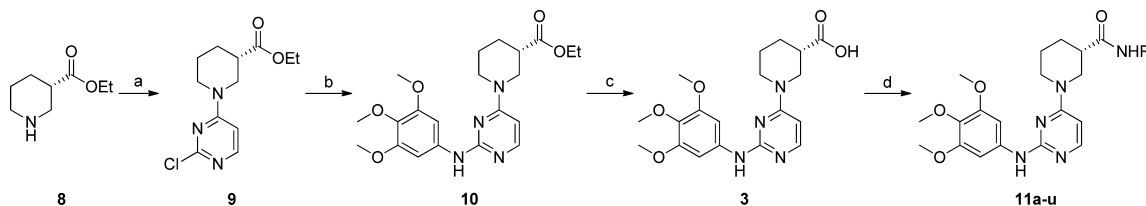
[a]Reagents and conditions: (a) 2,4-dichloropyrimidine, Et$_3$N, EtOH, 0–22 °C, 88%; (b) DMSO, 90 °C, 88%; (c) LiOH, H$_2$O, dioxane, 22 °C, quant; (d) Et$_3$N, HATU, DCE, 22 °C.

Scheme 4. Synthesis of R-Enantiomer of 1[a]
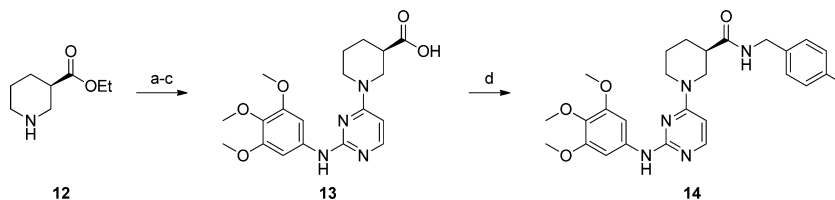
[a]Reagents and conditions: (a) 2,4-dichloropyrimidine, Et$_3$N, EtOH, 0–22 °C; (b) 3,4,5-trimethoxyaniline, DMSO, 90 °C; (c) TFA, CH$_2$Cl$_2$, 22 °C; (d) 5, HATU, Et$_3$N, CH$_2$Cl$_2$, 22 °C.

Table 1. Hinge Region Modifications

| compd | R | IC$_{50}$ (μM) ($\pm$SD)[a] | |
		ALK	IGF1R
1	3,4,5-OMePh	0.174 ($\pm$0.012)	4.61 ($\pm$0.75)
7a	Me	>25[c]	>25[c]
7b	Ph	2.32 ($\pm$0.13)[b]	>25[c]
7c	Bn	>25[c]	>25[c]
7d	3-ClPh	2.01 ($\pm$0.45)	>25[c]
7e	4-ClPh	6.30[c]	>25[c]
7f	3-OMePh	1.02 ($\pm$0.09)	9.022
7g	4-OMePh	3.10 ($\pm$2.06)	>25[c]
7h	3-EtPh	0.912 ($\pm$0.167)	>25[c]
7i	4-EtPh	>25[c]	>25[c]
7j	3,4-OMePh	1.73 ($\pm$1.31)	>25[c]
7k	3,4-benzodioxane	1.48 ($\pm$0.48)	>25[c]
7l	3,5-OMePh	0.325 ($\pm$0.173)[b]	2.93 ($\pm$1.20)[b]

[a]All values are the average of $n \geq 3 \pm$ standard deviation unless indicated otherwise. [b]$n = 2 \pm$ standard deviation. [c]$n = 1$.

proceeded without epimerization, as determined by chiral supercritical fluid chromatography (SFC).[21] Arrays of analogues were then rapidly assembled via S$_N$Ar reaction of 2 with various primary amines under thermal conditions. Final compounds were then obtained after high throughput mass-triggered preparative HPLC purification.[22]

The synthesis of intermediate 3 is outlined in Scheme 3. Reaction of 2,4-dichloropyrimidine with ethyl-(S)-nipecotate (8) following the procedure for intermediate 2 afforded pyrimidine 9. Coupling with 3,4,5-trimethoxyaniline under thermal conditions gave aniline 10, which was saponified with LiOH to generate carboxylic acid 3. HATU-mediated coupling of 3 with various amines proceeded with minimal racemization of the chiral center.[23] Final compounds were obtained as before

following high throughput mass-triggered preparative HPLC purification.[22]

In addition, the enantiomer of compound 1 (14) was generated from (R)-(−)-nipecotic acid ethyl ester (12) via carboxylic acid 13 using the method described for 3 (Scheme 4).

■ **RESULTS AND DISCUSSION**

Analogues were assayed for inhibition of ALK enzyme activity as well as selectivity over IGF1R.[24] ALK functional activity was measured using a time-resolved fluorescence resonance energy transfer (TR-FRET) assay which measured the phosphorylation of a peptide substrate.[11] FRET assays monitoring

Table 2. Amide Bond Modifications
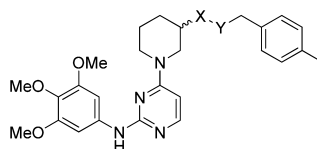
compd	X	Y	stereocenter	IC$_{50}$ (μM) ($\pm$SD)[a]	
				ALK	IGF1R
1	CO	NH	S	0.174 ($\pm$0.01)	4.61 ($\pm$0.75)
14	CO	NH	R	4.12 ($\pm$0.43)	>25

[a]All values are the average of $n \geq 3 \pm$ standard deviation.
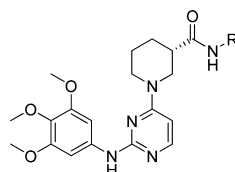
Table 3. Right-Hand Side Modifications

compd	R	IC$_{50}$ (μM) ($\pm$SD)[a]	
		ALK	IGF1R
1	−CH$_2$-(4-MePh)	0.174 ($\pm$0.012)	4.61 ($\pm$0.75)
11a	−Ph	0.833 ($\pm$0.063)	6.59[c]
11b	−CH$_2$-Ph	0.364 ($\pm$0.073)	6.12 ($\pm$0.75)[b]
11c	−(CH$_2$)$_2$-Ph	0.358 ($\pm$0.415)	>25[b]
11d	−(CH$_2$)$_3$-Ph	6.71 ($\pm$1.07)	6.39 ($\pm$1.17)[b]
11e	−CH$_2$-CO-Ph	2.94 ($\pm$0.83)	4.10
11f	−CH(S-Me)-Ph	2.60[c]	10.54[c]
11g	−CH(R-Me)-Ph	2.01[c]	>25[c]

[a]All values are the average of $n \geq 3 \pm$ standard deviation unless indicated otherwise. [b]$n = 2$. [c]$n = 1$.

Table 4. Right-Hand Side Substituent Effects
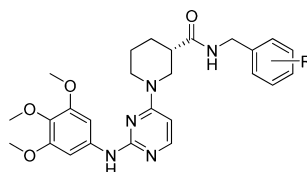
compd	R	IC$_{50}$ (μM) ($\pm$SD)[a]	
		ALK	IGF1R
1	4-Me	0.174 ($\pm$0.012)	4.61 ($\pm$0.75)
11h	2-Me	0.341 ($\pm$0.019)	8.32 ($\pm$2.62)[b]
11i	3-Me	0.083 ($\pm$0.018)	0.722 ($\pm$0.046)[b]
11j	3-OCF$_3$	0.016 ($\pm$0.001)[b]	0.116 ($\pm$0.015)[b]
11k	4-OCF$_3$	0.010 ($\pm$0.002)	0.798 ($\pm$0.088)[b]
11l	2-Cl	0.587[c]	7.08[c]
11m	3-Cl	0.080 ($\pm$0.040)	0.364 ($\pm$0.050)[b]
11n	4-Cl	0.095 ($\pm$0.012)	1.87 ($\pm$0.69)[b]
11o	3-NO$_2$	0.070 ($\pm$0.014)	0.503 ($\pm$0.062)[b]
11p	4-NO$_2$	2.93 ($\pm$0.59)	>25[b]
11q	3-CO$_2$Me	0.060 ($\pm$0.016)[b]	8.89 ($\pm$4.29)[b]
11r	4-CO$_2$Me	1.70 ($\pm$0.08)	>25[b]
11s	3-Ph	0.019 ($\pm$0.01)	4.23[c]
11t	4-Ph	0.138 ($\pm$0.026)	>25[b]
11u	3-OPh	0.192 ($\pm$0.054)	2.77 ($\pm$0.48)[b]

[a]All values are the average of $n \geq 3 \pm$ standard deviation unless indicated otherwise. [b]$n = 2$. [c]$n = 1$.

phosphorylation of a peptide substrate were also used for the counter-screening assay for IGF1R.

Structure−activity relationships specific to the hinge-binding region of the molecule are shown in Table 1, where

Table 5. Comparison of 1, 11q, and 11s in Enzyme and Cellular Assays
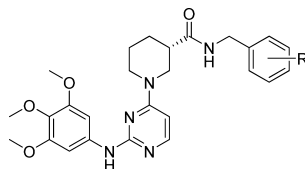
compd	R	cLogP	IC$_{50}$ (μM) ($\pm$SD)[a]		cell shift
			ALK	Karpas	
1	4-Me	4.24	0.174 ($\pm$0.012)	0.384 ($\pm$0.126)	2.2
11s	3-Ph	5.63	0.019 ($\pm$0.011)	0.224 ($\pm$0.122)	11.8
11j	3-OCF$_3$	4.77	0.016 ($\pm$0.001)[b]	0.059 ($\pm$0.021)	3.7
11m	3-Cl	4.46	0.080 ($\pm$0.040)	0.226[c]	2.8
11q	3-CO$_2$Me	3.71	0.060 ($\pm$0.016)[b]	0.061 ($\pm$0.032)	1.0
11v	3-morpholine	3.20	0.031 ($\pm$0.002)[b]	0.028 ($\pm$0.022)[b]	0.9

[a]All values are the average of $n \geq 3 \pm$ standard deviation unless indicated otherwise. [b]$n = 2$. [c]$n = 1$.

modifications generally resulted in a loss of potency. Replacement of the trimethoxyphenyl group with Me (**7a**) resulted in loss of detectible potency. An unsubstituted phenyl ring (**7b**) maintained measurable potency (IC$_{50}$ = 2.32 μM), although extending this group by one methylene unit (**7c**) was not tolerated. C-3 substitutions proved more potent than C-4 (**7d** vs **7e**, **7f** vs **7g**, **7h** vs **7i**), with 3-ethyl **7h** being the most potent (IC$_{50}$ = 0.912 μM). Disubstituted phenyl analogues such as 3,4-dimethoxyphenyl **7j** or 3,4-benzodioxane **7k** gave an order of magnitude loss in potency relative to **1** but were still active. 3,5-Dimethoxy analogue **7l** alone gave comparable potency (IC$_{50}$ = 0.325 μM) to **1**, most likely by mimicking the minimal interactions the meta-position methoxy groups make with the protein in the crystal structure. This also highlights the insignificance of the methoxy group at C-4, which projects into the solvent in the crystal structure. None of these modifications significantly impacted IGF1R selectivity.

Modification of the amide portion of piperidinyl carboxamide **1** proved detrimental to potency (Table 2). The *R*-enantiomer of compound **1** (**14**) was active, but less potent in the enzymatic assay (IC$_{50}$ = 4.12 μM) compared with the *S*-enantiomer. This finding is consistent with the interactions noted in the cocrystal structure where the carbonyl oxygen is hydrogen bonded to catalytic Lys1150 and the amide NH forms a hydrogen bond with the backbone carbonyl of Gly1269 (Figure 1A).[27]

Structure−activity relationships specific to the hydrophobic pocket are seen in Table 3. The spacing between the piperidine carboxamide and the pendant aryl ring as well as the substitution of the alkyl linker between these two moieties proved important for both ALK enzyme potency and selectivity. A direct linkage was tolerated (**11a**, IC$_{50}$ = 0.833 μM), although a one- or two-carbon tether length was preferred (**11b**, IC$_{50}$ = 0.364 μM, and **11c**, IC$_{50}$ = 0.358 μM, respectively). Further elongation of the tether (n = 3) gave an 18-fold loss in activity (**11d** vs **11c**). Substitution of the linker with either a carbonyl or methyl also negatively impacted potency (**11e** vs **11c**; **11f**,**11g** vs **11b**).

The effect of alternative phenyl substitution patterns on ALK potency is shown in Table 4. In general, substitution at the C-3 and C-4 positions was preferred over C-2 substitution. The C-2 methylated analogue **11h** was equipotent to the unsubstituted phenyl analogue **11b** (IC$_{50}$ = 0.341 μM vs IC$_{50}$ = 0.364 μM). Methylation at C-3 (**11i**, IC$_{50}$ = 0.083 μM) gave a 4-fold increase in potency relative to **1**, although a reduction in IGF1R

selectivity was observed (8-fold for **11i** vs 17-fold for **11b**). Introduction of a trifluoromethoxy group at C-3 or C-4 improved potency (**11j** IC$_{50}$ = 0.016 μM and **11k** IC$_{50}$ = 0.010 μM, respectively). As with **11i**, **11j** showed a decrease in selectivity over IGF1R. C-3 or C-4 halo-derivatives showed improved potency relative to C-2 (**11l**, **11m**, and **11n**), although C-3 analogue **11m** also exhibited increased activity for IGF1R. Strongly electron withdrawing groups such as nitro or methyl carboxylate maintained potency when appended to C3 (**11o** IC$_{50}$ = 0.070 μM and **11q** IC$_{50}$ = 0.060 μM, respectively) and decreased potency at C4 (**11p** IC$_{50}$ = 2.93 μM and **11r** IC$_{50}$ = 1.70 μM, respectively).

Appending a less electron-withdrawing, hydrophobic phenyl ring to the C3 position (**11s**) increased potency for ALK and improved selectivity over IGF1R (ALK IC$_{50}$ = 0.019 μM, IGF1R IC$_{50}$ = 4.23 μM) to give the most selective analogue identified in these studies. C4-substituted phenyl **11t** also maintained potency relative to methyl **1** (IC$_{50}$ = 0.138 μM vs IC$_{50}$ = 0.174 μM) without negatively impacting selectivity. Introduction of an ether spacer to **11s** (**11u**) led to a 10-fold loss in ALK potency and decreased IGF1R selectivity relative to **11s**.

The functional activity of piperidine carboxamide **1** and potent analogues **11j**, **11m**, **11q**, and **11s** was subsequently measured in an ALK-positive Karpas-299 whole cell assay (Table 5). An apparent correlation between cell shift and the calculated logP (cLogP) was observed, such that as cLogP increased (**11q** < **1** < **11m** < **11j** < **11s**), the cell shift also increased. These findings suggest that reducing clogP will lead to decreased cell shifts. To test this hypothesis, morpholine analogue **11v** was generated using the method described in Scheme 3. Gratifyingly, the resulting compound proved highly potent in the ALK enzyme and cellular assays (ALK IC$_{50}$ = 0.031 μM, cell IC$_{50}$ = 0.028 μM). To evaluate morpholine **11v** for kinase selectivity, the compound was analyzed in the IGF1R assay as well as tested at 1 μM against a panel of 99 kinases using the Ambit Biosciences KINOME*scan* platform.[25] Gratifyingly, morpholine **11v** was >200-fold selective over IGF1R (IC$_{50}$ = 7.39 μM) and showed no effect on IGF1R in the kinome panel. In addition, only 4 kinases, namely ALK, KIT, TRKA, and FLT3, have <30% percent-of-control (POC) for the compound. Compound **1** also showed activity toward these kinases as well as PAK2 and MAP2K5, with a POC <30% highlighting the improved selectivity of **11v**.[26]

CONCLUSIONS

In this investigation, a modular, parallel-synthesis approach was used to swiftly examine the hinge-binding region and hydrophobic pocket occupied by compound **1**, a selective ALK inhibitor. This approach allowed for rapid SAR development across different sections of the molecule concurrently and greatly increased the speed with which interesting and potent compounds were discovered. The SAR of this series of ALK inhibitors demonstrated that modification of the hinge-binding region fails to improve potency or selectivity. These findings are reasonable given that this part of the molecule is in a solvent-exposed region with minimal contacts to the protein outside of the linker binder. However, changes to the section of the molecule occupying the extended hydrophobic pocket created by an unusual DFG-shifted conformation were effective. Furthermore, we found that cellular potency correlated with the cLogP of the molecule and used these findings to generate morpholine **11v**, which was highly potent in both the ALK enzyme and cellular assays as well as selective over IGF1R and a broad range of kinases in a kinase scan. Tesaro, Inc. signed an agreement with Amgen granting Tesaro exclusive worldwide rights for the development, manufacture, commercialization, and distribution of small-molecule inhibitors of ALK. This work has established a path forward for the generation of more potent and selective ALK inhibitors currently underway.

EXPERIMENTAL DETAILS

General. All reagents and solvents were obtained from commercial suppliers and used without further purification. Silica gel chromatography was performed using prepacked silica gel cartridges (Biotage). ^{1}H NMR spectra were obtained on either a Bruker UltraShield 300 MHz or Bruker DRX 400 (400 MHz) spectrometer and reported as ppm downfield from the deuterated solvent. All tested compounds were purified to >95% purity at 215 and 254 nm as determined by HPLC. HPLC analysis was obtained on an Agilent 1100, using one of the following two methods: [A] Agilent SB-C18 column (50 mm × 3.0 mm, 2.5 μ) at 40 °C with a 1.5 mL/min flow rate using a gradient of 5−95% [0.1% TFA in acetonitrile] in [0.1% TFA in water] over 3.5 min; [B] Agilent Zorbax SB-C18 (50 mm × 3.0 mm, 3.5 μ) at 40 °C with a 1.5 mL/min flow rate using a gradient of 5−95% [0.1% TFA in acetonitrile] in [0.1% TFA in water] over 3.5 min. Enantiomeric excess was obtained by SFC using a Chiralpak AD-H column (4.6 mm × 15 cm, 5 um particle size) with carbon dioxide (gradient A) and methanol with 0.2% diethylamine (gradient B) as the mobile phase. A gradient of 5% B to 60% B for a run time of 7 min (40 °C, 4.0 mL/min, back pressure at 100 bar). The analysis software used were MassWare v. 4.01, MassLynx version 4.0 SP1 and Agilent LC/MSD Chemstation Rev.B.03.01. Exact mass (HRMS) measurements were performed on a Fourier-transform ion cyclotron resonance (FT-ICR) mass spectrometer operating at 7 T (Bruker Daltonics, Billerica MA). Ions were generated by electrospray ionization (positive mode). The instrument was externally calibrated with a PEG300/600 solution using the standard Francel equation. The calculated mass error for each calibrant ion was less than 1.0 ppm from the measured value. For each spectra 512 k data points were collected using a 1.25 MHz sweep width of detection. The time domain data were not processed prior to performing a magnitude mode Fourier transform.

(S)-tert-Butyl 3-(4-Methylbenzylcarbamoyl)-piperidine-1-carboxylate (6). To a solution of (S)-1-(tert-butoxycarbonyl)-piperidine-3-carboxylic acid (Beta Pharma Inc., 500 mg) and Et$_3$N (912 μL) in CH$_2$Cl$_2$ (11 mL) was added HATU (912 mg), followed by 4-methylbenzylamine (305 μL). The resulting solution was stirred at 23 °C for 48 h. The reaction was concentrated, and the residue was adsorbed onto a plug of silica gel and purified by chromatography through a 50 g silica gel column, eluting with 0.5−5% MeOH in CH$_2$Cl$_2$, to provide **6** (70% yield) as a white foam. ^{1}H NMR (300

MHz, CDCl$_3$) δ ppm 7.08−7.20 (m, 4 H), 6.13 (br s, 1 H), 4.38 (d, J = 5.26 Hz, 2 H), 3.92 (d, J = 13.30 Hz, 1 H), 3.62−3.83 (m, 1 H), 3.21 (dd, J = 13.01, 9.65 Hz, 1 H), 3.00 (dd, J = 10.40 Hz, 1 H), 2.33 (s, 3 H), 2.20−2.30 (m, 1 H), 1.80−1.95 (m, 2 H), 1.58−1.71 (m, 1 H), 1.43−1.52 (m, 1 H), 1.42 (s, 9 H). MS (ESI, positive ion) m/z: 355.2 [M + Na] 355.2.

(S)-1-(2-Chloropyrimidin-4-yl)-N-(4-methylbenzyl)-piperidine-3-carboxamide (2). To a solution of **6** (506 mg) in CH$_2$Cl$_2$ (15 mL) was added 1 M HCl in diethyl ether (8 mL). The reaction was maintained at 23 °C for 20 h while stirring. The reaction was concentrated to dryness and taken on to the next step without further purification. To a solution of the intermediate (409 mg) in EtOH (3 mL) was added 2,4-dichloropyrimidine (227 mg) and Et$_3$N (423 μL). The resulting solution was stirred at 23 °C for 20 h. The reaction was then concentrated and the residue was adsorbed onto a plug of silica gel and purified by chromatography through a 50 g silica gel column, eluting with 0.5−5% MeOH in CH$_2$Cl$_2$, to provide **2** (32% yield) as a white solid. ^{1}H NMR (300 MHz, CDCl$_3$) δ ppm 1.49−1.63 (m, 1 H) 1.74−1.85 (m, 1 H) 1.93−2.09 (m, 2 H) 2.29−2.43 (m, 4 H) 3.11−3.22 (m, 1 H) 3.57 (m, 1 H) 4.03 (m, 1 H) 4.18 (m, 1 H) 4.40 (m, 2 H) 6.40 (d, J = 6.28 Hz, 1 H) 7.14 (s, 4 H) 8.00 (d, J = 6.14 Hz, 1 H). ESI-MS [M + H] 345.0. 8.00 (d, J = 6.14 Hz, 1 H), 7.14 (s, 4 H), 6.40 (d, J = 6.28 Hz, 1 H), 4.40 (m, 2 H), 4.18 (m, 1 H), 4.03 (m, 1 H), 3.57 (m, 1 H), 3.11−3.22 (m, 1 H), 2.29−2.43 (m, 4 H), 1.93−2.09 (m, 2 H), 1.74−1.85 (m, 1 H), 1.49−1.63 (m, 1 H). MS (ESI, positive ion) m/z: 345.0 [M + H].

(S)-N-(4-Methylbenzyl)-1-(2-((3,4,5-trimethoxyphenyl)-amino)-4-pyrimidinyl)-3-piperidinecarboxamide (1). Intermediate **2** (86 mg) and 3,4,5-trimethoxyaniline (46 mg) were dissolved in DMSO (1 mL) and heated at 80 °C for 20 h. The reaction was cooled to 23 °C, diluted with water, and extracted with CH$_2$Cl$_2$ (2×). The combined organic layers were dried over Na$_2$SO$_4$, filtered, and concentrated. The crude material was absorbed onto a plug of silica gel and purified by chromatography through silica gel (10 g), eluting with 0.5− 5% MeOH in CH$_2$Cl$_2$, to provide **1** (65% yield) as a light-purple solid. ^{1}H NMR (400 MHz, CDCl$_3$) δ 7.95 (d, J = 6.06 Hz, 1H), 7.02− 7.17 (m, 5H), 6.83 (s, 2H), 6.36 (br s, 1H), 6.03 (d, J = 6.06 Hz, 1H), 4.26−4.43 (m, 2H), 4.22 (d, J = 12.32 Hz, 1H), 4.01 (br s, 1H), 3.74− 3.88 (m, 9H), 3.56 (dd, J = 9.29, 13.20 Hz, 1H), 3.14 (t, J = 10.47 Hz, 1H), 2.24−2.41 (m, 4H), 1.91−2.05 (m, 2H), 1.72 (dd, J = 4.30, 9.19 Hz, 1H), 1.46−1.61 (m, 1H). HRMS: calcd for (C$_{27}$H$_{33}$N$_5$O$_4$)H$^+$, 492.25978; found, 492.26004.

Preparation of 7a−l. General Procedure A. A mixture of the amine (435 μmol) and **2** (290 μmol) in DMSO (600 μL) was heated at 90 °C for 16 h. The mixture was then cooled to 23 °C, filtered through a course frit, and purified by mass-triggered preparative HPLC (Phenomenex Gemini-NX C18 110A column (100 mm × 21 mm, 5 μ), 44 mL/min flow rate, 5−95% [0.1% TFA in acetonitrile] in [0.1% TFA in water] over 10 min, mass spectral data were acquired from 100 to 850 amu in electrospray positive mode using MS, Waters SQ; UV, Waters 2487 or Waters PD) to provide the desired products as their TFA salts.

(S)-Ethyl 1-(2-Chloropyrimidin-4-yl)piperidine-3-carboxylate (9). To a solution of (S)-(+)-nipecotic acid ethyl ester (1 g) in EtOH (8 mL) was added Et$_3$N (885 μL), and the reaction was stirred at 23 °C. After 18 h, the reaction was concentrated and purified by chromatography through a 50 g silica gel column, eluting with 10− 90% ethyl acetate in hexanes, to provide the desired product (88% yield) as a clear oil. MS (ESI, positive ion) m/z: 270.0 [M + H].

(S)-Ethyl 1-(2-(3,4,5-Trimethoxyphenylamino)-pyrimidin-4-yl)piperidine-3-carboxylate (10). To a solution of **9** (9.5 g) in DMSO (70.1 mL) was added 3,4,5-trimethoxyaniline (6.4 g). The resulting solution was heated to 90 °C while stirring. After 3 d, the reaction was cooled to 23 °C and diluted with CH$_2$Cl$_2$. The organic phase was washed with water (3×). The combined aqueous layers were then extracted with CH$_2$Cl$_2$ (1×). The combined organic layers were then dried over sodium sulfate, filtered, and concentrated to give a residue. The residue was adsorbed onto a plug of silica gel and purified by chromatography through a 100 g silica gel column, eluting with 10−100% ethyl acetate in hexanes to provide **10** (88% yield) as

an off-white foam. ¹H NMR (300 MHz, CDCl₃) δ 7.98 (d, J = 5.99 Hz, 1H), 7.12 (s, 1H), 6.89 (s, 2H), 6.07 (d, J = 6.14 Hz, 1H), 4.38 (d, J = 12.86 Hz, 1H), 4.15 (q, J = 7.11 Hz, 3H), 3.78−3.90 (m, 10H), 3.28 (dd, J = 10.01, 13.08 Hz, 1H), 3.13 (t, J = 10.82 Hz, 1H), 2.47−2.59 (m, 1H), 2.11 (d, J = 8.92 Hz, 1H), 1.71−1.88 (m, 3H), 1.48−1.65 (m, 1H), 1.25 (t, J = 7.09 Hz, 3H). MS (ESI, positive ion) m/z: 417.1 [M + H].

(S)-1-(2-(3,4,5-Trimethoxyphenylamino)-pyrimidin-4-yl)-piperidine-3-carboxylic Acid (3). To a solution of **10** (1073 mg) in dioxane (9 mL) was added lithium hydroxide monohydrate (162 mg) in water (9 mL). The resulting reaction was stirred at 23 °C. After 1 h, the reaction was diluted with CH_2Cl_2 and washed with 1 N hydrochloric acid. The organic layer was extracted with aqueous sodium hydroxide. The aqueous layer was then acidified with 5 N hydrochloric acid to give a precipitate. The desired product was collected by suction filtration and air-dried to give **3** (86% yield) as a white solid. ¹H NMR (300 MHz, DMSO-d_6) δ ppm 10.49 (s, 1 H), 7.95 (d, J = 7.60 Hz, 1 H), 6.86 (s, 2 H), 6.69 (d, J = 7.60 Hz, 1 H), 3.98−4.21 (m, 1 H), 3.57−3.77 (m, 12 H), 2.53−2.64 (m, 1 H), 1.93−2.07 (m, 1 H), 1.65−1.86 (m, 2 H), 1.47−1.65 (m, 1 H). MS (ESI, positive ion) m/z: 389.1 [M + H].

Preparation of 11a−v. General Procedure B. To a solution of **3** (50 mg) in $ClCH_2CH_2Cl$ (1.5 mL) in a 24-well plate (Thomson Instrument Company) was added Et₃N (16 μL). To this mixture was added HATU (67 mg) in $ClCH_2CH_2Cl$ (1.0 mL) followed by the amine (353 μmol). The reaction plate was then sealed with a pierceable plate seal (Thomson Instruments) and shaken at 256 rpm on a variable speed mini vortex shaker (Eberbach Corporation) for 24 h. The reaction was diluted with MeOH (2 mL) and filtered. The filtrate was concentrated, and the reaction mixture was purified by mass-triggered preparative HPLC (Phenomenex Gemini-NX C18 110A column (100 mm × 21 mm, 5 μ), 44 mL/min flow rate, 5% to 95% [0.1% TFA in acetonitrile] in [0.1% TFA in water] over 10 min, mass spectral data were acquired from 100 to 850 amu in electrospray positive mode using MS, Waters SQ, UV, Waters 2487 or Waters PD) to provide the desired products as their TFA salts.

(S)-Methyl 3-((1-(2-(3,4,5-Trimethoxy-phenylamino)-pyrimidin-4-yl)piperidine-3-carboxamido)methyl)benzoate (11q). ¹H NMR (300 MHz, CDCl₃) δ ppm 7.81−7.92 (m, 3 H), 7.29−7.40 (m, 2 H), 6.92−7.19 (m, 1 H), 6.69−6.84 (m, 3 H), 6.06 (d, J = 6.28 Hz, 1 H), 4.29−4.51 (m, 2 H), 4.13 (dd, J = 13.59, 2.48 Hz, 1 H), 3.68−3.96 (m, 15 H), 2.39−2.52 (m, 1 H), 2.03−2.15 (m, 1 H), 1.89−2.03 (m, 1 H), 1.65−1.80 (m, 1 H), 1.49−1.65 (m, 1 H); HRMS: calcd for $(C_{28}H_{33}N_5O_6)H^+$, 536.24958; found, HRMS [M + H] 536.24978.

(S)-N-(3-Biphenylylmethyl)-1-(2-((3,4,5-trimethoxyphenyl)-amino)-4-pyrimidinyl)-3-piperidinecarboxamide (11s). ¹H NMR (400 MHz, CDCl₃) δ 7.48−7.60 (m, 4H), 7.32−7.47 (m, 4H), 7.13−7.26 (m, 1H), 6.82 (d, J = 6.06 Hz, 2H), 6.28−6.37 (m, 1H), 6.06−6.24 (m, 1H), 4.60−4.68 (m, 1H), 4.32−4.59 (m, 2H), 3.96 (d, J = 11.93 Hz, 1H), 3.72−3.85 (m, 9H), 3.50−3.67 (m, 1H), 3.16−3.39 (m, 1H), 2.37−2.51 (m, 1H), 1.74−2.13 (m, 5H), 1.42−1.69 (m, 1H). HRMS: calcd for $(C_{30}H_{38}N_6O_5)H^+$, 554.2762; found, 563.29729.

(S)-N-(3-(4-Morpholinyl)benzyl)-1-(2-((3,4,5-trimethoxyphenyl)amino)-4-pyrimidinyl)-3-piperidinecarbox-amide (11v). ¹H NMR (400 MHz, CDCl₃) δ 7.95 (d, J = 6.06 Hz, 1H), 7.27 (s, 1H), 7.19 (t, J = 7.82 Hz, 1H), 6.82 (s, 2H), 6.74−6.80 (m, 2H), 6.71 (d, J = 7.43 Hz, 1H), 6.48 (br s, 1H), 6.02 (d, J = 6.26 Hz, 1H), 4.35−4.43 (m, 1H), 4.22−4.32 (m, 2H), 3.80−3.84 (m, 10H), 3.78 (s, 3H), 3.44−3.57 (m, 1H), 3.06−3.13 (m, 5H), 2.35 (tt, J = 4.38, 9.02 Hz, 1H), 1.91−2.06 (m, 3H), 1.72 (td, J = 3.99, 13.35 Hz, 1H), 1.46−1.60 (m, 1H). HRMS: calcd for $(C_{32}H_{35}N_5O_4)H^+$, 563.29678; found, 563.29729.

ASSOCIATED CONTENT

Ⓢ Supporting Information

Synthesis of **7a−l**, **11a−p**, **11s−t**, and **14**, analytical data for final compounds, biological assay protocols, complete KINO-

ME*scan* results, and crystal structure information. This material is available free of charge via the Internet at http://pubs.acs.org.

Accession Codes

The cocrystal structure of ALK + **1** has been deposited in the RCSB (PDB ID 4DCE).

AUTHOR INFORMATION

Corresponding Author

*Phone: 617-444-5232. Fax: 617-577-9511. E-mail: richard.lewis@amgen.com.

Notes

The authors declare the following competing financial interest(s): The Authors are employees of Amgen Inc.

ACKNOWLEDGMENTS

ABBREVIATIONS USED

ALK, anaplastic lymphoma kinase; ALCL, anaplastic large-cell lymphoma; DCC, N,N'-dicyclohexylcarbodiimide; DCE, dichloroethane; DFG, Asp-Phe-Gly sequence in ATP binding site; FRET, fluorescence resonance energy transfer; HATU, 2-(7-aza-1H-benzotriazole-1-yl)-1,1,3,3-tetramethyluronium hexafluorophosphate; IGF1R, insulin-like growth factor-1 receptor; IMT, inflammatory myofibroblastic tumors; KIT, tyrosine−protein kinase (also known as CD117 or mast/stem cell growth factor receptor); PDB ID, protein data bank identity number; POC, percent of control; SAR, structure−activity relationship; SFC, supercritical fluid chromatography; TFA, trifluoroacetic acid; TR-FRET, time-resolved fluorescence resonance energy transfer

REFERENCES

(1) Palmer, R. H.; Vernersson, E.; Grabbe, C.; Hallberg, B. Anaplastic lymphoma kinase: signalling in development and disease. *Biochem. J.* **2009**, *420*, 345−361.

(2) Chiarle, R.; Voena, C.; Ambrogio, C.; Piva, R.; Inghirami, G. The anaplastic lymphoma kinase in the pathogenesis of cancer. *Nature Rev. Cancer* **2008**, *8*, 11−23.

(3) Mastini, C; Martinengo, C.; Inghirami, G.; Chiarle, R. Anaplastic lymphoma kinase: an oncogene for tumor vaccination. *Int. J. Mol. Med.* **2009**, *87*, 669−677.

(4) Lin, E.; Li, L; Guan, Y.; Soriano, R.; Rivers, C. S.; Mohan, S.; Pandita, A.; Tang, J.; Modrusan, Z. Exon Array Profiling Detects EML4-ALK Fusion in Breast, Colorectal, and Non-Small Cell Lung Cancers. *Mol. Cancer Res.* **2009**, *7*, 1466−1476.

(5) Mossé, Y. P.; Laudenslager, M.; Longo, L.; Cole, K. A.; Wood, A.; Attiyeh, E. F.; Laquaglia, M. J.; Sennett, R.; Lynch, J. E.; Perri, P.; Laureys, G.; Speleman, F.; Kim, C.; Hou, C.; Hakonarson, H.; Torkamani, A.; Schork, N. J.; Brodeur, G. M.; Tonini, G. P.; Rappaport, E.; Devoto, M.; Maris, J. M. Identification of ALK as a major familial neuroblastoma predisposition gene. *Nature* **2008**, *455*, 930−936.

(6) George, R. E.; Sanda, T.; Hanna, M.; Frohling, S.; Luther, W. II; Zhang, J.; Ahn, Y.; Zhou, W.; London, W. B.; McGrady, P.; Xue, L.; Zozulya, S.; Gregor, V. E.; Webb, T. R.; Gray, N. S.; Gilliland, D. G.; Diller, L.; Greulich, H.; Morris, S. W.; Meyerson, M.; Look, A. T. Activating mutations in ALK provide a therapeutic target in neuroblastoma. *Nature* **2008**, *455*, 975−978.

(7) Pulford, K.; Lamant, L.; Espinos, E.; Jiang, Q.; Xue, L.; Turturro, F.; Delsol, G.; Morris, S. The emerging normal and disease-related roles of anaplastic lymphoma kinase. *Cell. Mol. Life Sci.* **2004**, *61*, 2939−2953.

(8) Dirks, W. G.; Fahnrich, S.; Lis, Y.; Becker, E.; MacLeod, R. A. F.; Drexler, H. G. Expression and functional analysis of the anaplastic lymphoma kinase (ALK) gene in tumor cell lines. *Int. J. Cancer* **2002**, *100*, 49−56.

(9) Webb, T. R.; Slavish, J.; George, R. E.; Look, A. T.; Xue, L.; Jiang, Q.; Cui, X.; Rentrop, W. B.; Morris, S. W. Anaplastic lymphoma kinase: role in cancer pathogenesis and small-molecule inhibitor development for therapy. *Expert Rev. Anticancer Ther.* **2009**, *9*, 331−356.

(10) Kwak, E. L.; Bang, Y-J; Camidge, D. R.; Shaw, A. T.; Solomon, B.; Maki, R. G.; Ou, S-H I; Dezube, B. J.; Jänne, P. A.; Costa, D. B.; Varella-Garcia, M.; Kim, W-H; Lynch, T. J.; Fidias, P.; Stubbs, H.; Engelman, J. A.; Sequist, L. V.; Tan, W.; Gandhi, L.; Mino-Kenudson, M.; Wei, G. C.; Shreeve, S. M.; Ratain, M. J.; Settleman, J.; Christensen, J. G.; Haber, D. A.; Wilner, K.; Salgia, R.; Shapiro, G. I.; Clark, J. W.; Iafrate, A. J. Anaplastic Lymphoma Kinase Inhibition in Non-Small-Cell Lung Cancer. *N. Engl. J. Med.* **2010**, *363*, 1693−1703.

(11) Drew, A. E.; Al-Assaad, A. S.; Yu, V.; Andrews, P.; Merkel, P.; Szilvassy, S. J.; Emkey, R.; Lewis, R. T.; Brake, R. L. Comparison of two cell-based phosphoprotein assays to support screening and development of an ALK inhibitor. *J. Biomol. Screening* **2011**, *16* (2), 164−173.

(12) Iwahara, T.; Fujimoto, J.; Wen, D.; Cupples, R.; Bucay, N.; Arakawa, T.; Mori, S.; Ratzkin, B.; Yamamoto, T. Molecular characterization of ALK, a receptor tyrosine kinase expressed specifically in the nervous system. *Oncogene* **1997**, *14*, 439−339.

(13) Ullrich, A.; Gray, A.; Tam, A. W.; Yang-Feng, T.; Tsubokawa, M.; Colluns, C.; Henzel, W.; Le Bon, T.; Kathuria, S.; Chen, E.; Jacobs, S.; Francke, U.; Ramachandran, J.; Fujita-Yamaguchi, Y. Insulin-like growth factor I receptor primary structure: comparison with insulin receptor suggests structural determinants that define functional specificity. *EMBO J.* **1986**, *5*, 2503−2512.

(14) Gunby, R. H.; Ahmed, S.; Sottocornola, R.; Gasser, M.; Redaelli, S.; Mologni, L.; Tartari, C. J.; Belloni, V.; Gambacorti-Passerini, C.; Scapozza, L. Structural Insights into the ATP binding pocket of the anaplastic lymphoma kinase by site-directed mutagenesis, inhibitor binding analysis, and homology modeling. *J. Med. Chem.* **2006**, *49*, 5759−5768.

(15) Hendrickson, A. W.; Haluska, P. Resistance pathways relevant to insulin-like growth factor-1 receptor-targeted therapy. *Curr. Opin. Invest. Drugs* **2009**, *10*, 1032−1040.

(16) The cocrystal structure of ALK + **1** has been deposited in the RCSB (PDB ID 4DCE).

(17) Zuccotto, F.; Ardini, E.; Casale, E.; Angiolini, M. Through the "Gatekeeper Door": Exploiting the Active Kinase Conformation. *J. Med. Chem.* **2010**, *53*, 2681−2694.

(18) Lee, C. C.; Jia, Y.; Li, N.; Sun, X.; Ng, K.; Ambing, E.; Gao, M.-Y.; Hua, S.; Chen, C.; Kim, S.; Michellys, P.-Y.; Lesley, S. A.; Harris, J. L.; Spraggon, G. Crystal structure of the ALK (anaplastic lymphoma kinase) catalytic domain. *Biochem. J.* **2010**, *430*, 425−437.

(19) PDB ID 2OJ9.

(20) Velaparthia, U.; Wittman, M.; Liu, P.; Stoffan, K.; Zimmermann, K.; Sang, X.; Carboni, J.; Li, A.; Attar, R.; Gottardis, M.; Greer, A.; Chang, C. Y.; Jacobsen, B. L.; Sack, J. S.; Sun, Y.; Langley, D. R.; Balasubramanian, B.; Vyas, D. Discovery and initial SAR of 3-(1*H*-benzo[*d*]imidazol-2-yl)pyridin-2(1*H*)-ones as inhibitors of insulin-like growth factor 1-receptor (IGF-1R). *Bioorg. Med. Chem. Lett.* **2007**, *17*, 2317−2321.

(21) Supercritical fluid chromatography performed using Chiralpak IB (4.6 mm × 150 mm, 5μm) column and 35% methanol (with 0.2% DEA) as additive in supercritical CO_2. Total flow was 4 mL/min. Column temperature was kept at 40 °C and outlet pressure was controlled at 100 bar.

(22) Thomas, S.; Notari, S.; Semin, D.; Cheetham, J.; Woo, G.; Bence, J.; Schulz, C.; Provchy, J. Streamlined Approach to the Crude Compound Purification to Assay Process. *J. Liq. Chromatogr. Related Technol.* **2006**, *29*, 701−717.

(23) **11s** showed 10% racemization and **11a**, **11c**, **11d**, and **11i** showed ≤5% racemization by chiral SFC. All other compound showed a single enantiomer.

(24) A minimum significant ratio of 1.73 was calculated for the enzyme assays and 2.9 for the cellular assay.

(25) For more information, see *KINOMEscan*, a division of DiscoveRx, 11180 Roselle Street, San Diego, California 92121, United States; http://kinomescan.com/ (accessed Feb 7, 2012).

(26) For POC values for these compounds, refer to the Supporting Information.

(27) The sensitivity of the SAR of amide interaction with the protein indicates that the spatial disposition achieved in compound **1** is optimal. The coresponding 4-methylbenzyl ester **13** (cf. Table 2, X = CO; Y = O) is an order of magnitude less potent in the ALK enzyme assay (1.52 (± 0.253) μM), and reversal of the amide linkage as in compound **17** (cf. Table 2, X = NH; Y = CO), affords a compound devoid of measurable potency on the ALK enzyme.